Monthly Notices
of the
ROYAL ASTRONOMICAL SOCIETY

MNRAS **433,** 36–46 (2013)
Advance Access publication 2013 June 3

doi:10.1093/mnras/stt648

Irregular satellites of Jupiter: three-dimensional study of binary-asteroid captures

H. S. Gaspar,⋆ O. C. Winter⋆ and E. Vieira Neto⋆

UNESP – Univ. Estadual Paulista, FEG. Grupo de Dinâmica Orbital e Planetologia, Av. Dr. Ariberto Pereira da Cunha, 333, Guaratinguetá, SP, CEP 12.516-410, Brazil

Accepted 2013 April 15. Received 2013 April 14; in original form 2012 May 9

ABSTRACT

Among the hidden pieces of the giant puzzle, which is our Solar system, the origins of irregular satellites of the giant planets stand to be explained, while the origins of regular satellites are well explained by the *in situ* formation model through matter accretion. Once they are not locally formed, the most acceptable theory predicts that they had been formed elsewhere and became captured later, most likely during the last stage of planet formation. However, under the restricted three-body problem theory, captures are temporary and there is still no assisted capture mechanism which is well established. In a previous work, we showed that the capture mechanism of a binary asteroid under the co-planar four-body scenario yielded permanent captured objects with an orbital shape which is very similar to those of the actual prograde irregular Jovian satellites. By extending our previous study to a 3D case, here we demonstrate that the capture mechanism of a binary asteroid can produce permanent captures of objects by itself which have very similar orbits to irregular Jovian satellites. Some of the captured objects without aid of gas drag or other mechanisms present a triplet: semi-major axis, eccentricity and inclination, which is comparable to the already known irregular Jovian objects.

Key words: planets and satellites: formation.

1 INTRODUCTION

Irregular satellites are the majority of the planetary satellite population in the present Solar system. They are basically characterized by having large orbits, with high eccentricity and inclinations. Furthermore, it is possible to classify them into families with similar spectra and/or orbital shape (Nesvorný et al. 2003; Jewitt & Haghighipour 2007).

These peculiar characteristics suggest that these objects have not formed *in situ*, as the regular ones were (Lunine & Stevenson 1982; Vieira Neto & Winter 2001; Canup & Ward 2002, 2006; Mosqueira & Estrada 2003; Sheppard & Jewitt 2003; Deienno et al. 2011), but most likely captured at the final stage of planetary formation (Kuiper 1956; Colombo & Franklin 1971; Heppenheimer & Porco 1977; Pollack, Burns & Tauber 1979). However, the captures under the restricted three-body problem are temporary, and the existence of such objects depends on an auxiliary mechanism of capture.

Hence, many theories of such an auxiliary mechanism have been proposed. While some authors appeal to dissipative mechanisms, such as gas-drag effects (Pollack et al. 1979; Ćuk & Burns 2004; Vieira Neto & Winter 2009), others base their theories on interactive effects, such as the exchange reactions (Colombo & Franklin 1971; Tsui 1999, 2000; Astakhov et al. 2003; Nesvorný et al. 2003; Funato et al. 2004) and the pull-down mechanism (Heppenheimer & Porco 1977; Vieira Neto, Winter & Yokoyama 2004, 2006; Oliveira et al. 2007), for instance.

One of the most referenced works on the origin of irregular satellites is by Nesvorný, Vokrouhlický & Morbidelli (2007). Based on the Nice model of Solar system formation (Gomes et al. 2005; Morbidelli et al. 2005; Tsiganis et al. 2005), they show that the satellites may originate from the planetesimal disc throughout planetary encounters. However, they left the issue about the origin of Jovian irregular satellites open.

1.1 Milestones of the binary capture model

Agnor & Hamilton (2006) introduced the concept of a binary-asteroid capture in which a three-body gravitational encounter between a binary asteroid and a planet results in an orbital exchange reaction in such a way that one component of the primordial binary is kept bounded to the planet. In their work, they showed that Triton's capture likely resulted from a three-body gravitational encounter between a binary system and Neptune.

⋆E-mail: helton.unesp@gmail.com (HSG); ocwinter@feg.unesp.br (OCW); ernesto@feg.unesp.br (EVN)

Exploring the same idea, Vokrouhlický, Nesvorný & Levison (2008) and Nogueira, Brasser & Gomes (2011) studied the binary capture mechanism under the Nice model scenario. They followed an approach which is very similar to that of Agnor & Hamilton (2006), but adopted the planetesimal encounter trajectories from the Nice model as binary incoming trajectories. However, their binary capture study was performed under the three-body problem (planet-binary), neglecting the gravitational tidal field of the Sun in the planet's vicinity.

In agreement with the Agnor & Hamilton (2006) results, it is confirmed that Triton likely resulted from binary dissociation, but, additionally, Vokrouhlický et al. (2008) could estimate that such a capture should have happened very soon after Neptune's formation when the planetesimal disc was still dynamically cold.

They also pointed out that the binary dissociation was a highly unlikely process for the origin of small irregular satellites, since the orbital distribution of the captured bodies is inconsistent with that of the known irregular satellites, and also due to the low capture efficiency compared to the numerous populations of such objects.

Nogueira et al. (2011) have focused on Triton's case, demonstrating that its retrograde orbit went circularized which is very likely due to the tidal evolution. They left open the issue whether Triton was captured with a small semi-major axis at the same epoch as the other irregular satellites of Neptune, or before the dynamical instability of Nice's model.

Still in Triton's scope, it is fair to highlight the analytic approach by Kobayashi et al. (2012). Though they base their study on captures of binary stars by black holes, they devote some attention to the case of Triton's capture by Neptune.

Philpott, Hamilton & Agnor (2010) first published a work in which the Sun effect was considered. By focusing on the capture by Jupiter, they found that the energy loss from disruption was sufficient for capturing, but it could not directly deliver the bodies to the observed orbits of the actual irregular satellites.

Hence, they argued that the long-lived capture orbits could subsequently evolve inwards due to interactions with a tenuous circumplanetary gas disc. In a nutshell, their results were similar to those of Vokrouhlický et al. (2008).

Quillen, Hasan & Moore (2012) studied the probabilities of capture via binary disruptions under a scenario with two planets migrating due to interactions by an exterior cold planetesimal belt. They showed that the capture through binary interactions is statistically unlikely for inner giants, and also discussed an association of their model with exoplanets.

In our previous work (Gaspar, Winter & Vieira Neto 2011), we studied the capture mechanism of the binary asteroid under the four-body problem, taking Sun and Jupiter into account. We showed that the capture mechanism of the binary asteroids is capable of producing permanent captures of objects with an orbital shape that is very similar to the known Jovian prograde irregular satellites.

In that work, we explored many parameters and the most relevant mechanism intrinsic features were highlighted, which are important to obtain permanent captures.

The present work is an extension of a previous one (Gaspar et al. 2011). Hence, the next section summarizes the features of such a work which are extremely relevant to comprehend this study.

1.2 Highlights on the earlier study

1.2.1 Study for obtaining initial conditions

The first step was to obtain initial conditions under which a binary asteroid headed towards a close approach with Jupiter.

Such an issue was tackled using the three-body problem principle of reversibility. Designated as a capture-time study (Vieira Neto & Winter 2001), it consisted of setting up a grid of semi-major axis and eccentricity around Jupiter to integrate particles backwards in time for 10^4 yr.

A fraction of the particles collided with Jupiter and were not useful for the purpose of this previous work. Another fraction remained orbiting Jupiter during the whole integration time and were not useful for the aforementioned purpose either. A third fraction of particles escaped from Jupiter.

The system final state after the particle escape was taken as a *suitable initial condition*.

The heliocentric semi-major axis and the eccentricity are shown in Fig. 1. They were classified as long- or short-time suitable initial conditions, depending on whether the particle took more than 10^3 yr to escape from Jupiter or not, respectively.

Once the set of suitable initial conditions was obtained, a secondary asteroid was added around the primary one. For each suitable initial condition, 2400 initial conditions were generated by distributing the initial semi-major axis and the initial true anomaly of the secondary asteroid around the primary one. It was assumed that the binary asteroids were all initially circular and co-planar.

The semi-major axis and the true anomaly were distributed in a grid as $0.005\,r_{\rm H} < a < 1.000\,r_{\rm H}$ every $0.005\,r_{\rm H}$ and $0^\circ < f < 330^\circ$ every 30°, where $r_{\rm H}$ stands for the radius of Hill of the major component w.r.t. Sun.

1.2.2 Numerical approach

The binary capture process was divided into three main stages. Every binary asteroid is initially in a hyperbolic orbit around Jupiter and headed to a close approach with it. When the binary asteroid

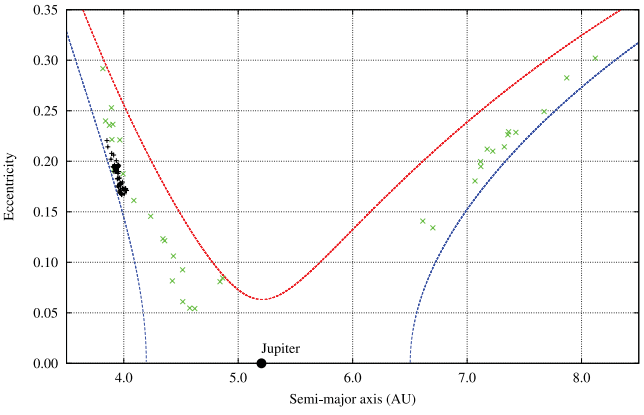

Figure 1. Suitable initial condition $a \times e$ heliocentric diagram. The green 'x' and black '+' stand for the short-time and long-time suitable initial conditions, respectively. The red and blue curves denote Tisserand's relations for $T = 2.996$ and 3.036, respectively, which encompasses all suitable initial conditions. Fig. 3 from Gaspar et al. (2011).

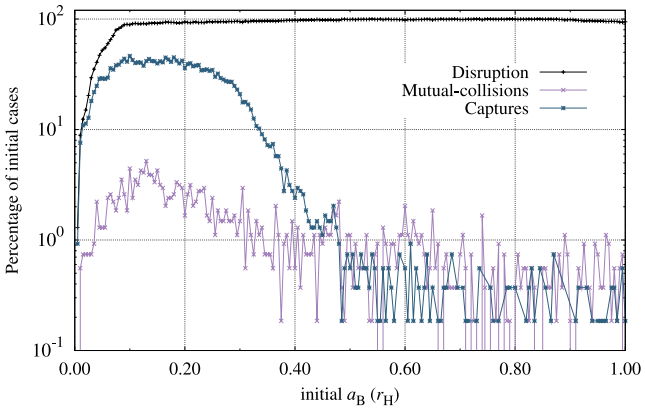

Figure 2. Histogram for the binary initial semi-major axis. The black curve represents the fraction of disrupted binaries as a function of the initial semi-major axis of the binary asteroid. Analogously, the blue curve represents the fraction of disrupted binary asteroids which remained captured. The violet curve shows the fraction of mutual collisions between the asteroids. Fig. 4 from Gaspar et al. (2011).

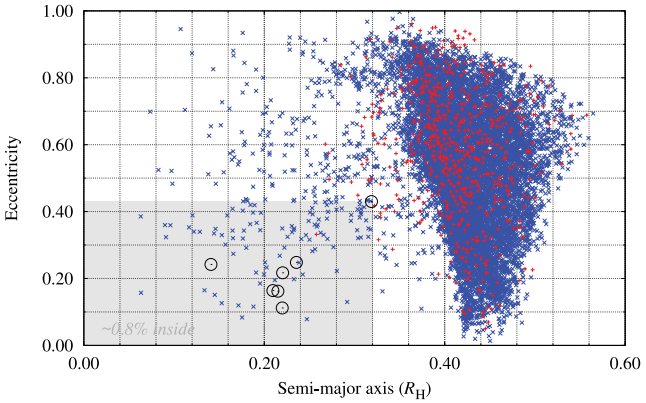

Figure 3. Diagram of the semi-major axis versus eccentricity of the captured asteroids. The black circumferences represent the orbital elements of Jupiter real prograde irregular satellites. The grey box roughly delimits the region occupied by the known actual prograde irregular satellites of Jupiter. It contains about 0.8 per cent of the captured objects. Fig. 9 from Gaspar et al. (2011). Semi-major axes are in units of the Hill radius of Jupiter.

is detected to be temporarily captured[1] by Jupiter, the first stage begins. Within this stage, the binary asteroid is either expected to disrupt, escape from Jupiter as a binary or mutually collide.

The last two outcomes are not worthy of interest, and the simulation is interrupted in such cases. At the instant in which the binary asteroid is dissolved, the second stage begins.

Depending on how the energy exchange happens, the resultant energy partition from the disruption process may provide the permanent capture of the component which loses energy, and a consequent escape of the component which gains energy.

After the component that gained energy escapes, the attention is focused on the one which remains captured during the third stage. During this last stage, the Jacob constant of the remaining asteroid is tracked.

This asteroid is considered as permanently captured if its Jacob energy value remains above the Lagrangian point L_1 Jacob energy for at least 10^2 yr.

1.2.3 Binary intrinsic features

By analysing the cases which resulted in permanent captures, we noted that the minor component of the binary asteroid is much more susceptible to permanent capture than the larger one.

Furthermore, the permanent capture probability, as a function of the binary initial separation, has an optimum separation value ($a_B \approx 0.15\, r_H$). When the binary initial separation value is lower than the optimum one, the binaries are so tight that they very frequently collide, as shown in Fig. 2. Beyond this optimum separation value, the permanent capture probability decreases as the binary separation increases because the initial binary separation constrains the amount of exchangeable energy.

These pieces of evidence indicate that the energy exchange plays a key role in the binary-asteroid capture process.

[1] The binary asteroid is considered temporarily captured when both asteroids two-body energy w.r.t. Jupiter are negative.

1.2.4 Mechanism intrinsic features constrained to the permanent captures

For the vast majority of cases in which the permanent capture occurred, it was observed that the binary asteroid entered the Hill sphere through the Lagrangian equilibrium point L_1.

Then, we noted that these incoming trajectories through point L_1 are those that come from long-time initial conditions. Long-time cases are those in which the particle took longer than 10^3 yr to escape from Jupiter's vicinity in the capture-time study backward integrations, which preferentially occurs when just a narrow bottleneck of the zero velocity curves is opened around L_1.

By analysing the angular disruption configuration for these permanent capture cases, it was observed that the binary asteroid enters the Hill sphere through L_1, and then disrupts after a quarter of its orbital evolution around Jupiter. Furthermore, the disruption configuration with the minor component between Jupiter and P1 is also a permanent capture preferable configuration, since the P2 orbital velocity around Jupiter is minimized in this configuration.

Fig. 3 shows the final orbital configuration of the permanent captured objects. The great majority of them are very far from the planet and must be removed by further perturbations that are not considered in this study.

The most important result is the fraction of 0.8 per cent of cases highlighted inside the grey box along with the actual prograde irregular Jovian satellites (black circumferences).

1.3 Present work main goal

As one can see in Fig. 3, object captures with an orbital shape which is very similar to the known prograde Jovian irregular satellites were achieved using the binary-asteroid capture mechanism for the first time, without the need of any other implement, such as gas dissipation for instance. However, these captures are not fairly comparable to the actual Jovian objects, since they do not have inclinations.

As previously mentioned, it was a preliminary study in which just the co-planar case was considered. Hence, it is quite justifiable to improve this study to a 3D case, considering the asteroid inclinations. Then, the main goal is to assess whether the binary-asteroid

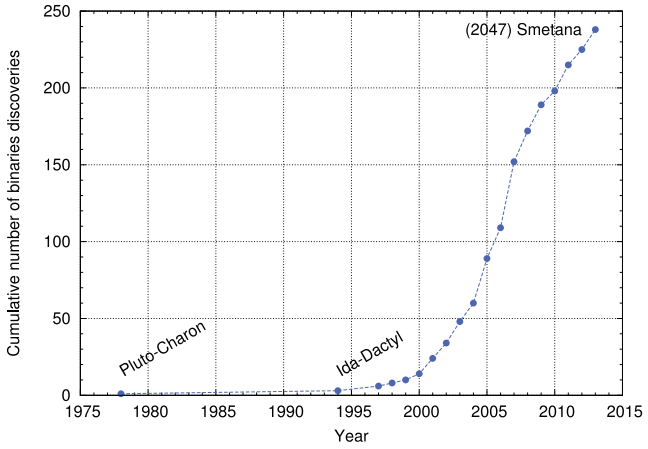

Figure 4. Discovery histogram of binary asteroids. (Source: Johnston 2013, http://www.johnstonsarchive.net; 2013 March 26.)

capture-dissociation process can generate captures by itself, with comparable orbits to the actual Jovian irregular satellites.

As an additional motivator, while double asteroid systems were taken as rare in the Solar system a few years ago, the total current amount of such systems surpasses the quantity of 200 objects (Johnston 2011), even facing the existing complexities in observing them (Noll et al. 2008). Fig. 4 highlights the increasing number of binary system discoveries.

We developed the present work by testing the hypothesis whether the observed orbits of actual irregular satellites of Jupiter can be explained via binary captures. To achieve this, the same approach of the previous work was used, but expanding the exploration of the initial condition space, giving particular attention to the binary separation and inclination.

Our approach will be discussed in detail in Section 2, followed by results and related discussions, shown in Section 3. The conclusions are summarized in Section 4.

In Appendix B (available as Supporting Information) we present detailed results of an aside study related to the adopted approach which is essential in supporting the present argumentation, and another one consisting of an inventory of Jupiter irregular satellites.

2 METHODOLOGY

One key feature of the present work is the conjecture that the energy exchange between the components of a binary asteroid can account for decreasing the orbital energy of one of the components, so that this component remains permanently bound after the binary disruption. The energy exchange also represents a variation on the orbital elements of the trapped body. Thus, in other words, the energy exchange must also account for a transition from an unstable region to a stable one within the $a \times e \times I$ space. Hence, a second key feature of this work is to explore the initial conditions in order to find those which lead the binary asteroid to the closest region to the stability border within the $a \times e \times I$ space.

2.1 Model

By following a very similar approach to the previous one (Gaspar et al. 2011), we considered the four-body problem dynamics with the Sun, Jupiter and a binary asteroid. The procedure considered the following: the binary asteroid initially orbits the Sun in a hyperbolic orbit headed to a close approach with Jupiter with low velocity. Thus, the binary asteroid becomes temporarily captured by Jupiter, i.e. it changes from the hyperbolic orbit to an elliptical one around Jupiter. The time instant of this temporary capture is labelled as T_1. Thus, at T_1, both asteroids have their two-body energy w.r.t. Jupiter with negative values. After the binary asteroid becomes temporarily captured, Jupiter tidal effects may cause its disruption. However, if the binary separation is sufficiently tight, the pair may remain mutually bound and escape from Jupiter as such. Such an outcome is defined as a *double escape*. On the other hand, widely separated binaries will be disrupted after a while at a time instant labelled as T_2. So, the wider the distance between the components, the easier the binary will be disrupted. After T_2, each member of the primordial binary orbits Jupiter independently in such a way that it can result in three possible outcomes.

(i) The asteroids may mutually collide[2]. We compute such cases as *mutual collisions*.

(ii) One asteroid may collide with Jupiter. We compute such cases as *collisions*.

(iii) One asteroid may escape from Jupiter, while its old partner remains captured at a time instant labelled as T_3.

For outcomes (i) and (ii), the simulation is interrupted, and the data are stored for future analysis. By following the dynamics, the simulation can result in three possible outcomes after instant T_3.

(i) The remaining asteroid may collide with Jupiter. We also compute such cases as *collisions*.

(ii) The remaining asteroid may escape from Jupiter, resulting in a *successive escape*.

(iii) The remaining asteroid is considered as *permanently captured* if it matches one of the following orbital conditions for at least 10^2 yr:

$$\begin{cases} I \leq 70^\circ \\ e < 1 \\ Q \leq 0.48\, R_{\rm H} \end{cases} \quad \text{or} \quad \begin{cases} I \geq 110^\circ \\ e < 1 \\ Q \leq 0.69\, R_{\rm H}, \end{cases} \tag{1}$$

where I, e and Q are the captured asteroid inclination, eccentricity and apojove distance, respectively, and $R_{\rm H}$ stands for the Jupiter Hill radius, whose referred fractions are well-established limits for prograde (Domingos, Winter & Yokoyama 2006) and for retrograde moons (Hamilton & Krivov 1997; Nesvorný et al. 2003).

The cases with inclinations within the Kozai–Lidov range (70°: 110°) are neglected. It is known that Kozai–Lidov resonance effects remove objects orbiting within such a range of inclination (Carruba et al. 2002; Nesvorný et al. 2003; Yokoyama et al. 2003).

2.2 Primary initial conditions

The described model depends on the suitable initial conditions in order for the binary asteroid to be headed to a close approach with Jupiter. These suitable initial conditions were obtained from the *capture-time study* (Vieira Neto & Winter 2001) analogously to our previous work, as described in Section 1.2.1. In this work, as well as in the work by Vieira Neto & Winter (2001), the planet eccentricity is 0.

Although the capture-time study was performed in order to obtain the suitable initial conditions in this work, its main result is a capture-time map[3] as a function of the particle initial orbital

[2] Actually, mutual collisions can occur at any time of the process.

[3] It mainly maps the stable and unstable regions of the $a \times e$ space around the planet (Vieira Neto & Winter 2001).

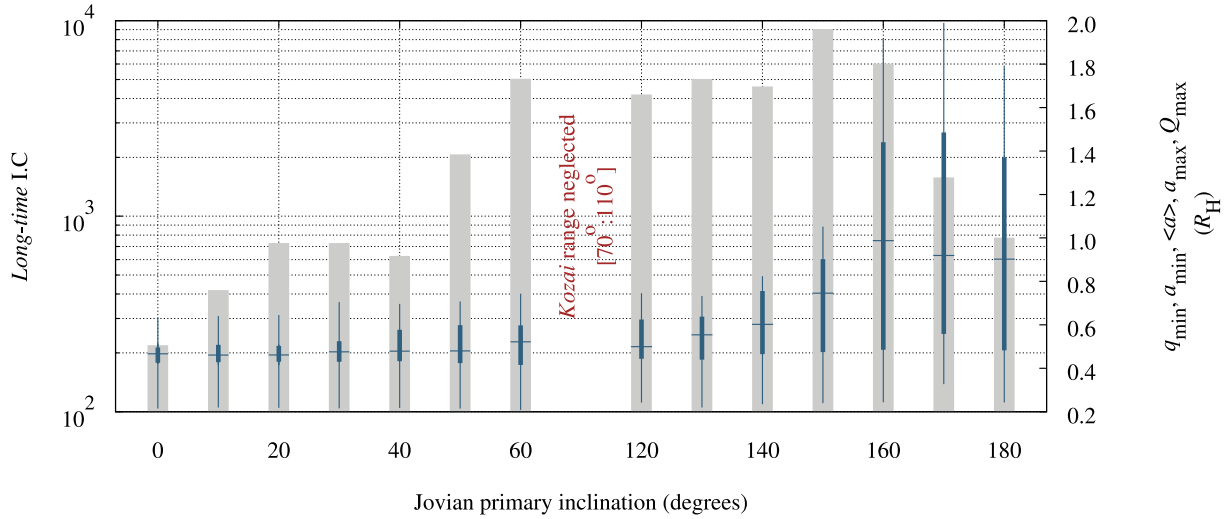

Figure 5. Summarized data of the *capture-time study* of Appendix B (available as Supporting Information). The grey boxes denote the amounts of long-time cases obtained for each primary initial inclination. Analogously, the thin blue bar extremities stand for minimum perijove and maximum apojove among all of the test particles with the respective primary inclination. The thick blue line extremities stand for minimum and maximum values of the semi-major axis, and the plus signs denote the mean values of the semi-major axis. Elements with length dimension are in the right scale.

elements around the planet (Vieira Neto & Winter 2001; Domingos et al. 2006). In this work, we performed the capture-time study for test particles' primary initial inclination ranging from 0° to 60°, varying in 10° for the prograde case, and from 120° to 180°, varying in 10° for the retrograde case. The generated maps are shown in Appendix B (available as Supporting Information).

Fig. 5 summarizes the relevant data of such capture-time maps. The remarkable feature of this histogram relates to the distinct amounts of long-time cases obtained for each inclination. In this work, only the long-time cases were dealt with. As highlighted in Section 1.2.4, the long-time initial conditions are the most efficient in producing permanent captures. Short-time cases have such a negligible permanent capture probability that, in order to look for trajectories which get very close to Jupiter, would increase the degree of complexity of the present study by an expendable gain. Fig. 5 still depicts the minimum, medium and maximum values of the semi-major axis relative to each inclination, and it reveals the extension of the primary initial condition orbital space. Note that, when the space is more extended, it implies a lower surface density of primary initial conditions, as observed for the majority of the retrograde cases.

2.3 Suitable initial conditions

As previously explained, the suitable initial conditions were obtained by integrating the primary initial conditions backwards in time. In order to standardize the study over all the inclinations, we adopted the same number of initial conditions for each inclination. Based on the amount of cases for 10° inclination, 400 cases were chosen with the longest capture time among the long-time capture cases. With the exception of the zero inclination case, only 219 cases were able to be adopted. The suitable initial condition distribution in the heliocentric $a \times e \times I$ space is shown in Fig. 6(a). As already highlighted in Gaspar et al. (2011), this distribution conveys notable features. (i) Tisserand's mean values ∼3 indicate that the incoming trajectories have enough slow speed to account for the captures while matching real objects, for instance, the external border of the main belt. (ii) Objects are sufficiently far from Jupiter in order not to be accreted during its formation, while a tiny perturbation can change their orbits in order to lead them to a close encounter with Jupiter. (iii) Capture of objects coming from the Hilda family is in agreement with the results by Ćuk & Burns (2004). In order to have a quantitative idea about these suitable initial conditions, Fig. 6(b) shows the corresponding histograms.

2.4 Binary-asteroid modelling

In order to create the binary asteroid using the suitable initial conditions, we added a second asteroid orbiting the particle from the capture-time study. The major and secondary components of the binary asteroid will be referred to as P1 and P2 from now on, respectively, and the orbital elements of P2 w.r.t. P1 will be referred to as binary elements. P1 and P2 masses are $m_1 = 10^{20}$ and $m_2 = 10^{19}$ kg, respectively. Note that the Himalia mass, the largest irregular satellite of Jupiter, is about 10^{19} kg (Emelyanov 2005). From each of the suitable initial conditions, 160 binary asteroids were generated by distributing their semi-major axis from $0.005\,r_H$ up to $0.800\,r_H$ in steps of $0.005\,r_H$. The initial binary eccentricity is 0, and its initial inclination w.r.t. the ecliptic plane is uniformly distributed within the 0°:180° interval. The binary initial longitude of ascending node (Ω) and true anomaly (f) are also uniformly distributed within the 0°:360° interval.

2.5 Numerical approach details

The numerical simulations were performed by using a Gauss–Radau-based numerical integrator (Everhart 1985), and their accuracy was verified by checking the total system energy conservation. It was found that the energy fluctuations did not surpass 10^{11}. The Jacob constant of the binary barycentre was also monitored before its disruption, and it was found that C_J fluctuations remained lower than 10^9.

Storing data for the integration of each trajectory for 10^4 yr would demand a huge disc space, besides an unfeasible work to analyse them. In order to avoid the storage of a large amount of data, a monitoring routine was implemented to check the system state at

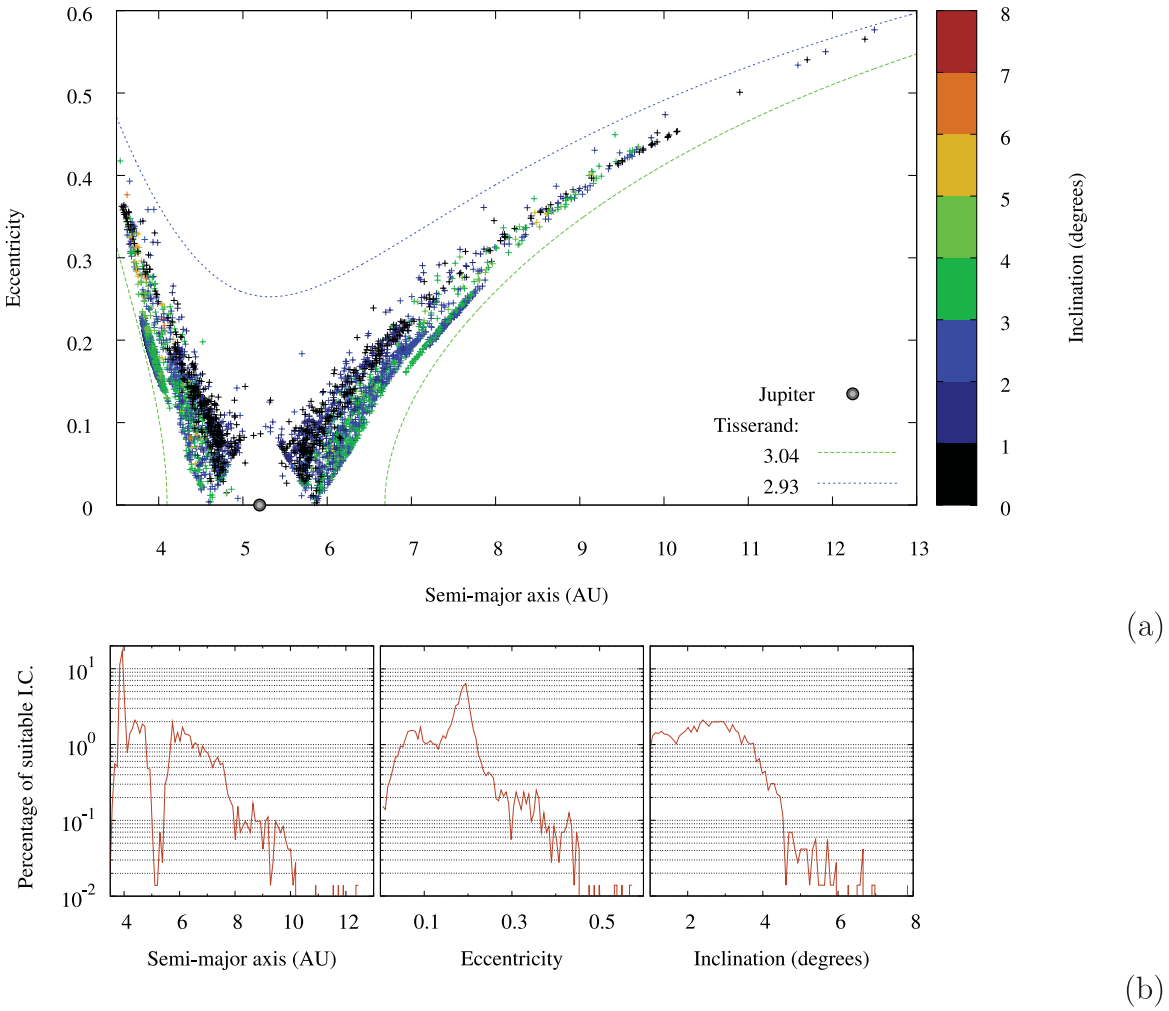

Figure 6. Suitable initial conditions which will generate the initial conditions of the primary asteroid. Plot (a) shows the heliocentric initial $a \times e \times I$ space, and the colour scale matches the inclinations. The dashed curves denote the Tisserand calculation for $I = 4°$, the mean value of the inclinations range. Plot (b) shows the heliocentric suitable initial condition a, e and I histograms.

every output step. This monitor determines instants T_1, T_2 and T_3, and it stores only a snapshot of the system state for each of these instants.

3 RESULTS

3.1 Results tied to the suitable initial conditions

This section contains the result analysis tied to the adopted suitable initial conditions, and the following discussion addresses the orbital inclination distribution of the captured objects.

Fig. 7 shows the inclination histogram of the captured objects. Since the amounts of initial conditions were equal for all suitable initial inclinations, except the case when $I = 0°$, the non-uniform distribution reveals some preferable inclinations. In the case of prograde inclinations, it can be seen that the maximum capture rate occurs for ranges between 20° and 40°, being in agreement with the actual distribution of prograde Jovian irregular satellites, since five out of seven are within this range, as one can see in Table A1.

Now, as for the retrograde cases, it can be seen that the inclination distribution of the captured objects does not match the distribution of actual Jovian irregular satellites. Fig. 7 shows the highest amount for the range 120°:130°, where none of the known Jovian irregular satellites are found. Furthermore, taking into account that more than 8×10^5 simulations were performed, this histogram reveals low capture efficiency. Nevertheless, we obtained very good captures in terms of the orbital configuration, as will be discussed in Section 3.3, and also it must be noted that the results were obtained by using a rigorous criterion of capture (see conditions 1), i.e. many pseudo-capture cases were discarded in which one component of the binary remained bound in a close orbit, but did not match the capture criteria. Indeed, the blue bars and crosses in Fig. 7 highlight that the average orbital shape of the captured objects reasonably matches the actual irregular satellites well.

In fact, the greatest result featured by this histogram is elucidated along with the analysis of the capture-time maps of Appendix B (available as Supporting Information). By comparing the histogram with such maps, we comprehend that the capture amount distribution as a function of the inclinations is not an intrinsic feature of the mechanism, but rather a reflection of the employed initial conditions, according to the following explanation.

By looking into the binary close approach scenario, the binary incoming trajectory is expected to be very similar to the escape pathway drawn by the particle in the capture-time study in an opposite direction, however. Hence, the binary closest approach with

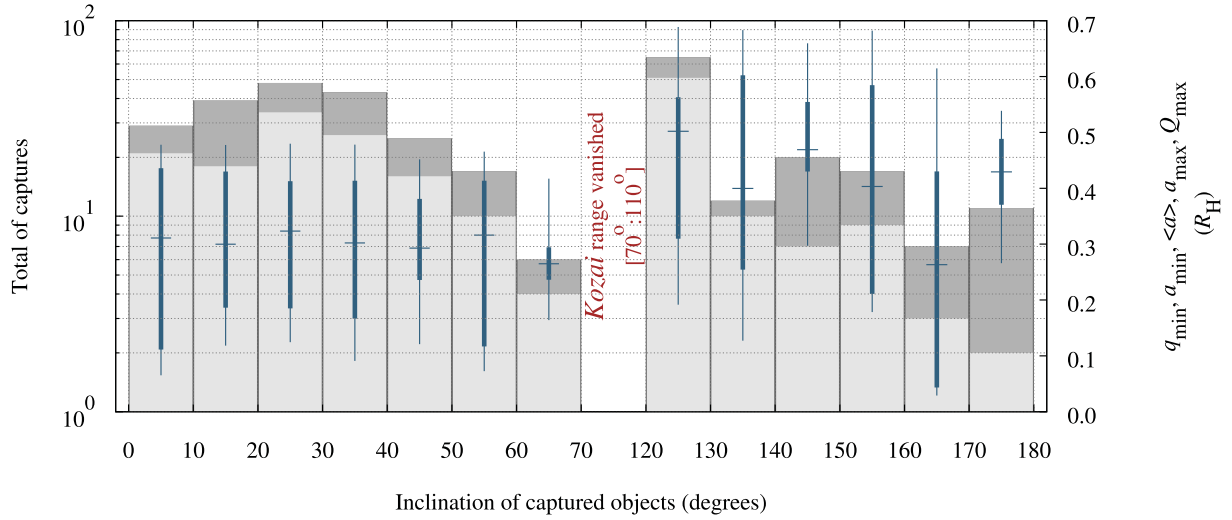

Figure 7. Summarized data of the captured objects. Analogous to Fig. 5 but for linearly binned inclinations of the permanently captured objects (see conditions 1). Additionally, the light-grey boxes stand for the fraction with $e \leq 0.5$.

Jupiter is expected to be very similar to the primary initial condition of the test particle. Thus, the binary will disrupt during its close approach by dropping its components in a state which is quite similar to that of the primary initial condition. However, the exchanges of energy and the angular momentum between the binary components will account for delivering the component which loses energy into a stable orbit around the planet, while the binary component which gains energy will escape (see fig. 5 of Gaspar et al. 2011).

Once convinced by such an explanation, the analysis of the capture-time maps of Appendix B (available as Supporting Information) is done. The maps show that the long-time primary initial conditions are distributed along the border between the stable and the short-time regions. Consequently, the combined region of stability, close C_J and stable in Figs B1 and B2, correlates with the primary semi-major axis distribution, i.e. the less extended the combined region, the smaller is the average primary semi-major axis. For instance, for the case $I = 120^\circ$, there are long-time initial conditions (blue dots) with $a = 0.55\,R_H$ ($e = 0.1$), as can be seen in Fig. B2, while for the case $I = 150^\circ$, the smallest a for long-time initial conditions (blue dots) is $0.8\,R_H$ ($e = 0.1$). Therefore, as expected, the smaller the semi-major axis, the more suitable are the initial conditions to produce good captures.

In Fig. 7, for the case of the retrograde captures, it was noted that the inclination distribution presents a trend of decreasing amounts of capture, as the inclinations increase. By looking at Fig. B2, along with the inclinations increasing, a trend of increasing regions of stability is noted. Therefore, it seems that there is a correlation showing that the capture amounts decrease as the size of the stable regions increases.

Hence, we conclude that the inclination distribution in Fig. 7 is a consequence of the adopted approach to obtain the suitable initial conditions. Therefore, it is not fairly comparable to the inclination distribution of the known Jovian irregular satellites. Indeed, better results would likely be achieved if the suitable initial conditions could be obtained from the primary initial conditions, taken from within the stable regions (dark areas in Fig. B2). However, by using the three-body model to obtain the suitable initial conditions, as we have done, the stable regions cannot be used, i.e. a test particle with a primary initial condition within the stable region will never escape from Jupiter and, consequently, will never generate a suitable initial condition. Therefore, we speculate that better suitable initial conditions could be obtained by including perturbations which would shrink the stable regions. It was not taken into account in the present work because it would substantially increase the degree of complexity of the problem. However, such issues are currently being studied for future works. Nevertheless, we show in Section 3.3 a set of captured objects on very similar orbits to the known irregular Jovian satellites achieved just by using the current model, without the need of any dissipative effect.

3.2 Results tied to the binary modelling

Along the previous section, the resultant implications from the assumptions on the suitable initial conditions were discussed. From now on, the resultant effects from binary modelling will be focused. First, we verified that permanent capture cases do not have apparent correlations with the binary mutual inclination.[4] Therefore, any graphics relative to such a quantity were suppressed. Thus, since the binary is initially in a circular orbit, the dependence on the binary separation should be analysed.

By following the same analysis, as in the previous work shown in Fig. 2, we analyse the outcome distributions as a function of the binary initial semi-major axis in Fig. 8. The current disruption distribution presents the same profile as the previous one. As expected, many tight binaries are kept bound[5] after their encounter with Jupiter. As the binary separation increases, the disruption phenomena tend to reach 100 per cent, as well. The distribution profile of mutual collisions is also similar to the previous one, but it presents a maximum value of collisions relative to a smaller binary separation, as a consequence of the additional degree of freedom. Pseudo-captured objects are those trapped due to zero velocity curves which close at L_1, but they do not satisfy the current capture criteria. It is the capture definition adopted in the previous work, but the current pseudo-capture distribution in Fig. 8 presents a profile that is quite different from the previously obtained one (Fig. 2), i.e. the current decaying rates as the function of the binary separation are

[4] Orbital inclination of P2 around P1 w.r.t. the ecliptic plane.
[5] Tidal forces do not cause its disruption.

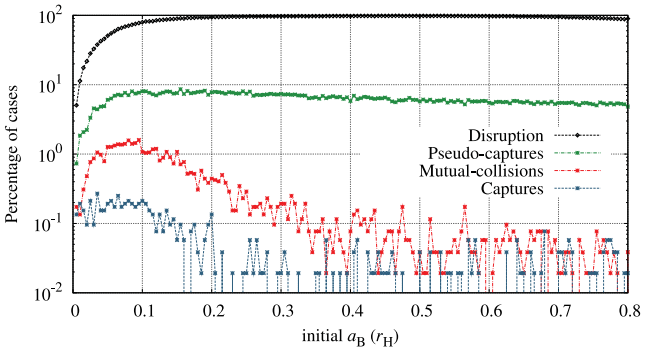

Figure 8. Outcome histograms as a function of the binary initial semi-major axis. The black curve stands for the fractions of disrupted binaries. The red curve stands for the fractions of collisions, while the blue and green curves denote the percentage of genuine and pseudo-captures, respectively. The genuine ones mean the captured objects obey the conditions of criteria (1), while the pseudo-captures stand for the cases in which the objects were trapped by the zero velocity curves, though they did not obey the capture criteria. The semi-major axis scale is given in units of P1 initial Hill's radius, and the percentage is relative to the number of simulated cases for each value of the binary semi-major axis.

shallow. Since the available exchangeable potential energy is only a function of the binary initial separation, such shallow decaying indicates that the current necessary energy exchange to keep an object captured in an inclined orbit is inferior compared to the co-planar case. Evidently, the additional freedom degree does not change, nor the planetocentric radial distance or the planetocentric velocity of the captured object. However, a new acceleration component which is perpendicular to the ecliptic plane arises. Such additional acceleration aggregates a new term to the Jacob energy variation, causing the zero velocity curves to close at the Lagrangian point L_1 more easily than in the co-planar case. On the other hand, though a smaller amount of exchangeable energy accounts for the necessary Jacob energy variation in the 3D case, the necessary decrease of the semi-major axis to satisfy the capture criteria is not accomplished.

The genuine capture distribution is similar to that of the co-planar case. It has a maximum amount value tied to an optimum binary separation. Very tight binaries more frequently survive the temporary capture by Jupiter and, on the other hand, the rate of permanent capture decreases as the binary initial separation increases because such a separation constrains the available exchangeable energy, i.e. the wider the binary separation, the lesser is the exchangeable energy. However, the current maximum value is two orders of magnitude inferior to that of the co-planar case, and the current binary optimum separation is about half the value of the previous one. It is also a consequence of the current capture criteria, i.e. in order to satisfy the current capture criteria, the necessary binary exchangeable energy constrains an initial binary separation threshold which is lesser than the previous one. Indeed, note that, in the previous work, many of the captured objects had a very large semi-major axis, analogously to the current pseudo-captures (see Fig. 2).

3.3 Final configuration of captured objects

The plots of Figs 9 and 10 present the final orbital configuration of the captured asteroids, in terms of the osculating semi-major axis, eccentricity and inclination for prograde and retrograde orbits, respectively. The known irregular satellites of Jupiter were also included in these plots in order to compare the results. Both figures were trimmed above $e > 0.5$ to make the comparison with the actual

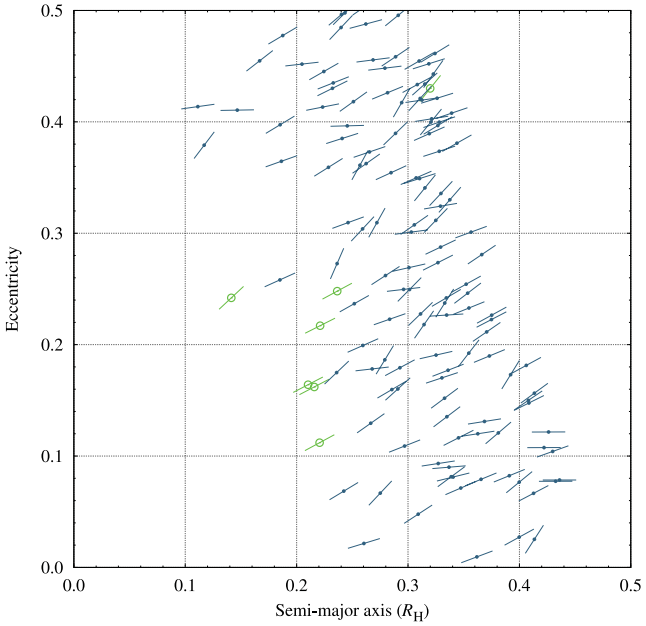

Figure 9. The blue colour represents the prograde captured objects. The tilted solid bars stand for inclination. Analogously, the green set stands for the actual irregular satellites of Jupiter.

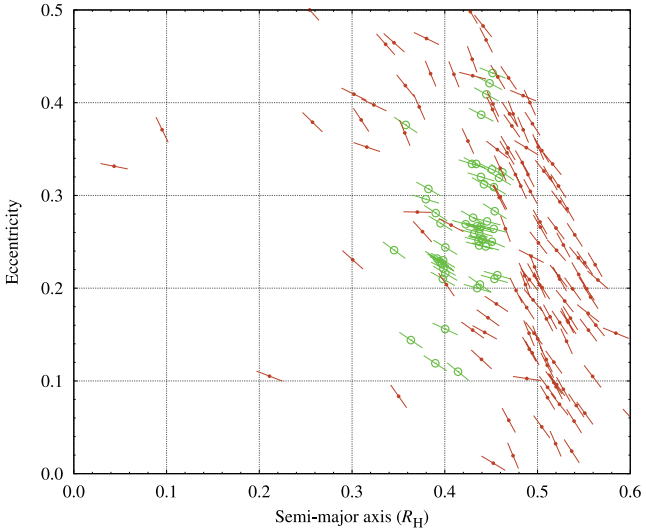

Figure 10. The red colour represents the retrograde captured objects. The tilted solid bars stand for inclination. Analogously, the green set stands for the actual irregular satellites of Jupiter.

satellites easier. Furthermore, the $a \times e \times I$ diagrams of pseudo-capture cases were suppressed. It was verified that such pseudo-captures present an orbital distribution which is very similar to that observed in Fig. 3 for $0.36\,R_H \lesssim a \lesssim 0.52\,R_H$.

Fig. 9 shows that there are some dozens of simulated objects captured on orbits which are very similar to some of the actual irregular satellites. The prograde captured objects fill a large range of eccentricity and inclination, but their semi-major axes are slightly distributed outermost in comparison to the actual ones. See also, in Appendix C (available as Supporting Information), the a, e and I cumulative distributions of the captured objects. This is still a consequence of the adopted initial conditions. As was discussed in Section 3.1, the capture state is expected to be quite similar

to the primary initial condition, and the semi-major axis decrease must be accomplished by an energy loss, i.e. the binary mutual energy exchange must account for the difference between the capture semi-major axis and the primary initial semi-major axis. Since the average primary initial semi-major axes are substantially greater in comparison to the actual ones, the energy exchange must be really expressive in order for the object to suffer a substantial semi-major axis decrease, and become captured into the region of the known Jovian irregular satellites. Indeed, there are a small fraction of captured objects that seem to satisfy such a condition. There are some objects that are close to the known Jovian objects. Particularly, there are good correspondences to Carpo, being the most external and eccentric.

By looking at Fig. 10, it can be seen that the simulated retrograde captured objects are also vastly distributed in eccentricity. As shown in Fig. 7, the inclinations cover the whole spectrum. Some captured objects with eccentricity that is greater than 0.5 have good final inclinations, but they are far from the actual satellites in the $a \times e$ space, and they are not shown here. As with the prograde captures, the semi-major axis of the captured retrograde objects is also slightly outermost, and this is also a consequence of the adopted initial conditions. As summarized in Fig. 5, the mean values of the semi-major axis are high in the capture-time maps, according to the inclinations that are greater than 140°, in Fig. B2. Thus, in order for an object with such a primary initial inclination to become captured within the region of the known Jovian irregulars, a large decrease of the semi-major axis is expected, as a consequence of the binary disruption. Such a large semi-major axis variation demands a large amount of exchangeable energy, but it happens with a lower probability. The two retrograde objects captured with the semi-major axis smaller than 0.1 R_H in Fig. 10 are examples of such rare kinds of captures. Note that such rare cases of capture followed by an eccentricity dumping could be an explanation for the origin of Triton (Nogueira et al. 2011).

Closer looks of Fig. 9 are shown in Figs 11 and 12. It shows that some captured objects have their final orbital elements which are

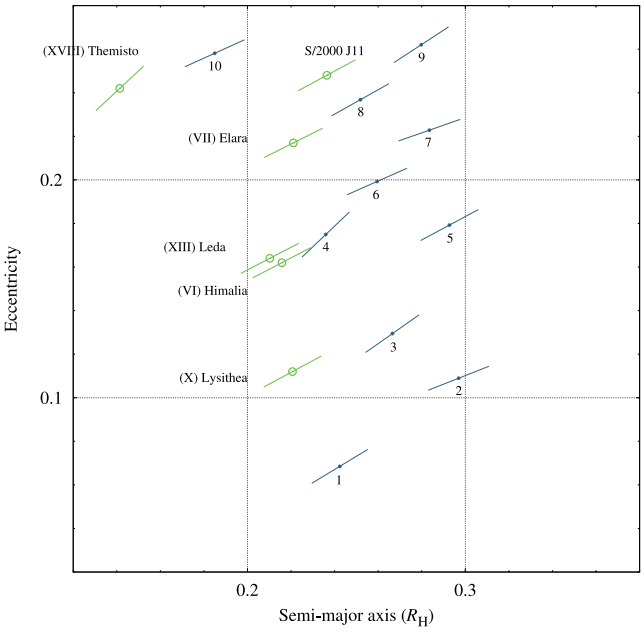

Figure 11. Closer look of Fig. 9 showing some of the actual satellites and some captured objects.

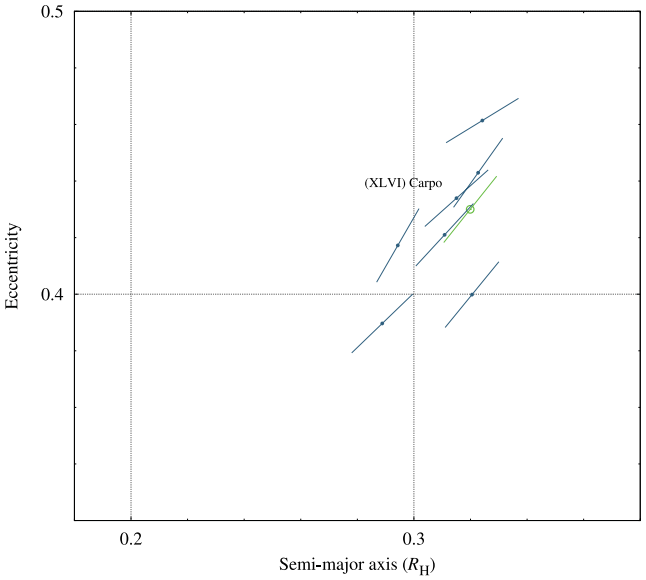

Figure 12. Closer look of Fig. 9 showing (XLVI) Carpo and some of the captured objects.

similar to the actual satellites. In Fig. 11, we can see that satellites 1, 2 and 3 are very close to (X) Lysithea in the $a \times e$ space, and satellite 1 also has quite the same inclination. Although satellite 4 has a different inclination from (VI) Himalia and (XIII) Leda, it has the values of the semi-major axis and an eccentricity which is close to those satellites. The inclination of these two satellites can be compared with captured objects 2, 5 and 6. Even captured object 1, which has an eccentricity that is lower than Himalias and Leda's, could have its distance compared. Captured object 3 can also be compared with (XVIII) Themisto. Captured objects 8 and 9 could be (VII) Elara and S/2000 J11. Finally, we note that the triangle formed by 1, 9 and 10 delimits a region with all actual satellites, but Themisto, with very close inclinations.

Fig. 12 shows (XLVI) Carpo with some captured objects. In this case, the coincidence is much greater. Three captured objects which are very close to Carpo in the $a \times e$ space can be seen, although the inclinations are not so close. But there is a captured object with eccentricity 0.4 which has inclination and semi-major axis values that are very close to Carpo's. Most absolutely, with an increase in the number of simulations, this result could be improved and, just by chance, a much closer satellite to Carpo's position would be found (semi-major axis, eccentricity and inclination).

Fig. 13 shows a closer look of Fig. 10. There are some well-positioned captured objects, such as number 8 and S/2003 J3, and mainly captured object 7 which quite matches S/2003 J16 orbital elements. Captured objects 1, 2, 3 and 4 delimit the region which encloses (XLV) Helike, (XXXIV) Euporie, S/2003 J18 and S/2003 J15. The quadrilateral formed by captured objects 5, 6, 7 and 8 covers a region of the $a \times e$ space, with similar inclinations which comprehend the whole Ananke Group, part of the Carme Group, (L) Herse, S/2003 J41, S/2003 J5 and S/2003 J10. Captured objects 9 and 10 could form the Pasiphae Group, or they could be satellite S/2010 J2. Captured object 11 resembles S/2011 J2, (VIII) Pasiphae, (XIX) Megaclite, or even (XXVIII) Autonoe. Although the inclinations do not match very well, captured objects 12, 13 and 14 are close to S/2003 J12.

As can be seen in the figures shown in this section, the simulations obtained a considerable number of captured objects around the a,

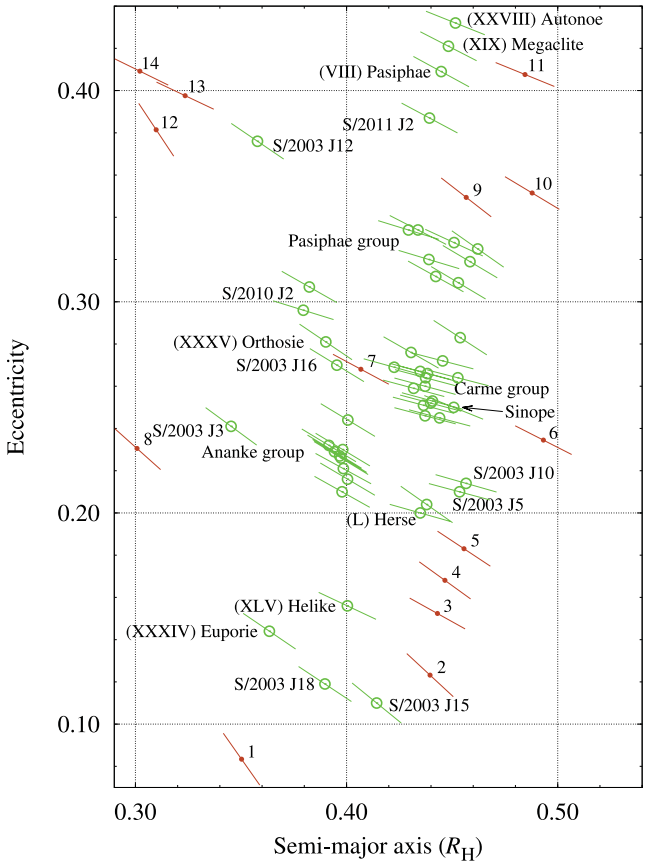

Figure 13. Closer look of Fig. 10 showing the actual satellites and some captured objects.

e, I position of the actual satellites of Jupiter. If the simulations continue, cases like Carpo in Fig. 12 will happen again, as some captured objects enclosing regions with the actual satellites are seen and, by chance, at some moment, another object could be captured with very comparable a, e, I orbital elements to the actual satellites. The results also show that most objects are captured on high eccentric and/or distant orbits, and do not correspond to any of the existing known irregular satellites. By the imposed criteria of capture, these objects are stable and could also be driven to orbits that are similar to the actual irregular Jovian satellites via further effects (Philpott et al. 2010; Nogueira et al. 2011). However, it is out of the scope of this paper to assess such conjecture, since it is focused on verifying the capacity of the binary-asteroid disruption process in generating captures of objects by itself in similar orbits to the known Jovian irregular satellites.

4 CONCLUSION

In this work, the four-body model with binary-asteroid disruption was used to investigate the possibility of a dynamical formation of the irregular satellites of Jupiter. The initial conditions were generated using the three-body model with orbits around Jupiter, and choosing the ones with the longest time to escape from Jupiter. Binary asteroids were built up and put along the obtained trajectories by changing the time integration direction. The binary asteroids were captured by Jupiter, disrupted while in a close approach to Jupiter. In this process, one escaped and the other one remained as an irregular satellite. In Section 3.1, it can be seen that it is very difficult to statistically analyse the results because an important region of retrograde orbits is not accessible through the three-body problem. In spite of this difficulty, the most important result was highlighted in Section 3.3 by the fraction of captured objects whose orbital configurations well match to those of the known Jovian irregular satellites. These were obtained without the use of any other mechanisms to reduce semi-major axis value, eccentricity or inclination, as other well-known theories of formation of irregular satellites need to.

For instance, in Fig. 13, it is noted that captured objects 10, 11, 13, 14 and 7 present very close inclinations to those of Pasiphae Group, and are also spread in a region of the $a \times e$ space that encompasses with almost the whole Pasiphae Group. The energy exchange occurring from the disruption of the binary asteroid is enough to reduce the semi-major axis of the captured component. To match the eccentricity and the inclination of the actual satellites, it is necessary to use out-of-plane capturing trajectories, and with slow velocity, as performed in this work. It may look restrictive, but Fig. 6 shows that those conditions are normally found in known asteroids.

The capture mechanism of the binary-asteroid study is still in progress, and there are many issues yet unaddressed. Nevertheless, after the work by Nesvorný et al. (2007), the present work is the very first one to show the final configuration of captured objects in terms of *semi-major axis versus eccentricity versus inclinations* comparable to the known Jovian irregular satellites, and obtained without the need of any other artefact, such as dissipation for instance.

ACKNOWLEDGEMENTS

We gratefully acknowledge CNPq, FAPESP and CAPES, which have funded this work. The suggestions and questions from the referee Ramon Brasser which helped us to improve this paper and the FDCT – Foundation for the Scientific and Technological Development – for the English editing support.

REFERENCES

Agnor C. B., Hamilton D. P., 2006, Nat, 441, 192
Astakhov S. A., Burbanks A. D., Wiggins S., Farrelly D., 2003, Nat, 423, 264
Canup R. M., Ward W. R., 2002, AJ, 124, 3404
Canup R. M., Ward W. R., 2006, Nat, 441, 834
Carruba V., Burns J. A., Nicholson P. D., Gladman B. J., 2002, Icarus, 158, 434
Colombo G., Franklin F. A., 1971, Icarus, 15, 186
Ćuk M., Burns J. A., 2004, Icarus, 167, 369
Deienno R., Yokoyama T., Nogueira E. C., Callegari N., Santos M. T., 2011, A&A, 536, A57
Domingos R. C., Winter O. C., Yokoyama T., 2006, MNRAS, 373, 1227
Emelyanov N., 2005, A&A, 438, L33
Everhart E., 1985, in Carusi A., Valsecchi G. B., eds, Astrophysics and Space Science Library, Vol. 115, Proc. IAU Colloq. 83, Dynamics of Comets: Their Origin and Evolution. Reidel, Dordrecht, p. 185
Funato Y., Makino J., Hut P., Kokubo E., Kinoshita D., 2004, Nat, 427, 518
Gaspar H. S., Winter O. C., Vieira Neto E., 2011, MNRAS, 415, 1999
Gomes R., Levison H. F., Tsiganis K., Morbidelli A., 2005, Nat, 435, 466
Hamilton D. P., Krivov A. V., 1997, Icarus, 128, 241
Heppenheimer T. A., Porco C., 1977, Icarus, 30, 385
Jewitt D. C., Haghighipour N., 2007, ARA&A, 45, 261
Johnston W. R., 2011, NASA Planetary Data System, 147
Johnston W. R., 2013, Asteroids with Satellites, available at: http://www.johnstonsarchive.net/astro/asteroidmoons.html#2
Kobayashi S., Hainick Y., Sari R., Rossi E. M., 2012, ApJ, 748, 105
Kuiper G., 1956, Vistas Astron., 2, 1631

Lunine J. I., Stevenson D. J., 1982, Icarus, 52, 14
Morbidelli A., Levison H. F., Tsiganis K., Gomes R., 2005, Nat, 435, 462
Mosqueira I., Estrada P. R., 2003, Icarus, 163, 198
Nesvorný D., Alvarellos J. L., Dones L., Levison H. F., 2003, AJ, 126, 398
Nesvorný D., Vokrouhlický D., Morbidelli A., 2007, AJ, 133, 1962
Nogueira E. C., Brasser R., Gomes R., 2011, Icarus, 214, 113
Noll K. S., Grundy W. M., Chiang E. I., Margot J.-L., Kern S. D., 2008, Binaries in the Kuiper Belt. University of Arizona Press, Tucson, p. 345
Oliveira D. S., Winter O. C., Vieira Neto E., de Felipe G., 2007, Earth Moon Planets, 100, 233
Philpott C. M., Hamilton D. P., Agnor C. B., 2010, Icarus, 208, 824
Pollack J. B., Burns J. A., Tauber M. E., 1979, Icarus, 37, 587
Quillen A. C., Hasan I., Moore A., 2012, MNRAS, 425, 2507
Sheppard S. S., Jewitt D. C., 2003, Nat, 423, 261
Tsiganis K., Gomes R., Morbidelli A., Levison H. F., 2005, Nat, 435, 459
Tsui K., 1999, Planet. Space Sci., 47, 917
Tsui K., 2000, Icarus, 148, 139
Vieira Neto E., Winter O. C., 2001, AJ, 122, 440
Vieira Neto E., Winter O. C., 2009, Math. Probl. Eng., 2009, 1
Vieira Neto E., Winter O. C., Yokoyama T., 2004, A&A, 414, 727
Vieira Neto E., Winter O. C., Yokoyama T., 2006, A&A, 452, 1091
Vokrouhlický D., Nesvorný D., Levison H. F., 2008, AJ, 136, 1463
Yokoyama T., Santos M. T., Cardin G., Winter O. C., 2003, A&A, 401, 763

SUPPORTING INFORMATION

Additional Supporting Information may be found in the online version of this article:

Appendix A. Inventory of Jovian irregular satellites.
Appendix B. Capture-Time maps.
Appendix C. Comparing orbital elements distributions (http://mnras.oxfordjournals.org/lookup/suppl/doi:10.1093/mnras/stt648/-/DC1)

Please note: Oxford University Press are not responsible for the content or functionality of any supporting materials supplied by the authors. Any queries (other than missing material) should be directed to the corresponding author for the article.

This paper has been typeset from a TEX/LATEX file prepared by the author.